

P. S Tofts
N. C Silver
G. J. Barker
A. Gass

Object strength - an accurate measure for small objects that is insensitive to partial volume effects

Received: 22 February 2005
Revised: 27 April 2005
Accepted: 3 May 2005
Published online: ■
© ESMRMB 2005

P. S. Tofts (✉) · N. C. Silver
G. J. Barker · A. Gass
Institute of Neurology,
University College London,
Queen Square, London
WC1N 3BG, UK
E-mail: p.tofts@ion.ucl.ac.uk;
Tel: +44-7837-3611 ext 4301
Fax: +44-7278-5616

N. S. Silver
Walton Centre for Neurology and
Neurosurgery,
Lower Lane, Liverpool L7 9LJ, UK

G. J. Barker
Centre for Neuroimaging Sciences,
Department of Neurology, Box 089,
Institute of Psychiatry,
Kings College London,
De Crespigny Park,
London SE5 8AF, UK

A. Gass
Departments of Neurology/Neuroradiology,
Universitätsklinikern,
Kantonsspital Basel, Petersgraben 4,
4031 Basel, Switzerland

Introduction

Quantitative measurements of small objects (either lesions or structures such as fibre tracts, the optic nerve or spinal cord), where the voxel size is comparable with the object size, are nearly always subject to error from partial volume effects. Whether the aim is to measure the object size (as is frequently required for lesions in clinical trials [1]), or to measure the mean value of an MR parameter (e.g. mean

Abstract There are currently four problems in characterising small nonuniform lesions or other objects in Magnetic Resonance images where partial volume effects are significant. Object size is over- or under-estimated; boundaries are often not reproducible; mean object value cannot be measured; and fuzzy borders cannot be accommodated. A new measure, Object Strength, is proposed. This is the sum of all abnormal intensities, above a uniform background value. For a uniform object, this is simply the product of the increase in intensity and the size of the object. Biologically, this could be at least as relevant as existing measures of size or mean intensity. We hypothesise that Object Strength will perform better than traditional area measurements in characterising

small objects. In a pilot study, the reproducibility of object strength measurements was investigated using MR images of small multiple sclerosis (MS) lesions. In addition, accuracy was investigated using artificial lesions of known volume (0.3–6.2 ml) and realistic appearance. Reproducibility approached that of area measurements (in 33/90 lesion reports the difference between repeats was less than for area measurements). Total lesion volume was accurate to 0.2%. In conclusion, Object Strength has potential for improved characterisation of small lesions and objects in imaging and possibly spectroscopy.

Keywords Lesion volume · Imaging · Spectroscopy · Multiple sclerosis · MRI · Partial volume · Brightness area product

magnetisation transfer ratio (MTR) in the optic nerve), voxel size limits what is possible. We report work stimulated by the need to improve between-centre agreement in reporting of the MTR values of multiple sclerosis lesions, after a standardised method of image data collection had been established [2].

The principle error is that object size may be over- or under-estimated, depending on the strategy of the observer, and on the object size and contrast. In a study on

	1033400106	R	Despatch: 6.7.2005	Journal : 10334	No. of Pages : 8
	Journal No. Manuscript No.		Author's Disk received <input checked="" type="checkbox"/>	Used <input checked="" type="checkbox"/>	Corrupted <input type="checkbox"/>

realistic artificial lesions of volume 0.3–6.2 ml the mean error was about 17%, and depended very much on the observer and the lesion contrast [3].

The second error is that estimates of the mean value in the object are likely to be biased towards the value of the surrounding normal tissue, since many partial voxels are included in the estimate of the mean. Thus lesions with abnormally low intensity values (dark lesions) would have mean values that are over-estimates of the intrinsic value for that lesion, depending on the size of the lesion. Conversely bright lesions would have mean values that are underestimates. Using a smaller ROI reduces the partial volume error, but at the expense of increased errors from noise and tissue heterogeneity (if present).

A third problem that may be encountered in studying small lesions is that observers may differ in their strategies on where to place a region of interest (ROI) that defines the border of the lesion, since the border is indistinct, giving rise to poor reproducibility. All three problems arise from the partial volume effect, and one approach is to pursue smaller voxel size; however the signal-to-noise ratio (or the scanning time) deteriorates rapidly, with little gain in spatial resolution. Even with better RF coil design or higher field strength, the gains in spatial resolution are relatively small.

A fourth source of error is that some lesions have biologically indistinct borders, as well as an intrinsically heterogeneous composition. For example lesions of multiple sclerosis may show episodic reactivation [4]. In this case concepts such as lesion volume or mean signal intensity in a lesion lose their meaning, regardless of voxel size.

In this work we pursue a different approach, where voxel size is almost irrelevant, and lesions can have fuzzy borders. The total ‘strength’ of the lesion, or of any small object, relative to its background, is measured. Qualitatively, this may be understood (for a uniform three-dimensional (3D) object) as being the product of the excess signal (i.e. the amount by which it exceeds the background signal, which is assumed uniform) and the volume of the object. Thus if the object is blurred by the imaging process, this product is unaffected. The exact positioning of Regions of Interest (ROI’s) becomes unimportant, provided the whole object has been included.

Object Strength (OS) is here formally defined, for the first time, as the integral of the excess signal intensity over the whole extent of the object, (which need not be uniform, although it should ideally be everywhere brighter or everywhere darker than the background). This can be measured in one slice (in which case we only obtain part of the object’s strength; the whole is obtained by summing the contributions from all the slices that contain part of the object); or in principle it could be computed directly from a three-dimensional image dataset. The method was implemented manually,

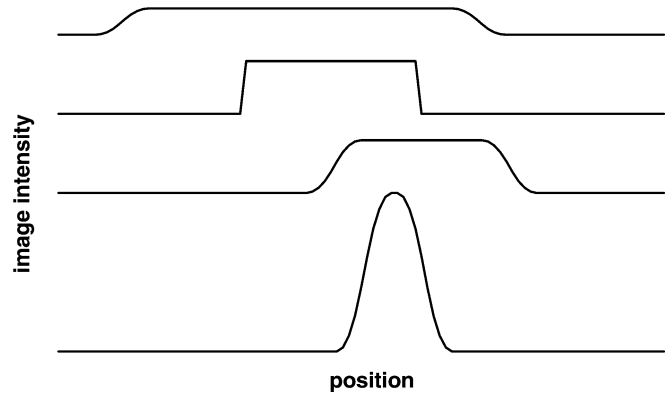


Fig. 1 Examples of one-dimensional objects that all have the same object strength or Total EXcess Intensity (TEXI)

in two dimensional MR images, for an initial evaluation.

Some one-dimensional objects that all have the same object strength are shown in Fig. 1. These show the variety in size, peak intensity, mean intensity, edge sharpness and object uniformity that can occur, and can be accommodated within the concept of Object Strength.

Lesions have often been characterised by their size or by the mean value of an MR parameter within the lesion. The product of excess signal and object size is a biologically plausible parameter to characterise abnormal tissue, since it combines measures of how abnormal the tissue is and how much tissue is affected. For example in the case of MTR reduction, a greater loss probably indicates more severe tissue destruction, and a larger volume indicates a greater amount of damaged tissue.

In small multiple sclerosis lesions the reproducibility of object strength measurements was found to be comparable with that of lesion volume measurements. The accuracy of the method, using images of artificial OCCA [3] lesions of known volume, was found to be better than for area measurements. Preliminary accounts of this work have already been presented [5, 6].

Theory

The Object Strength of a small blurred (3D) object on a uniform background is formally defined as the volume integral of its excess intensity over all space:

$$S^{\text{obj}} = \int (I^{\text{obj}}(r) - I^{\text{bgd}}) dV \quad (1)$$

The excess intensity is the amount by which its intensity $I^{\text{obj}}(r)$ at position r exceeds that of the background I^{bgd} . The integration is taken over enough space such that the whole object is included. The expectation value of the integral (i.e. its value in the absence of noise) is then independent of the exact limits of integration, since regions of pure

background, (where $\langle I_{\text{obj}}(\mathbf{r}) \rangle = I_{\text{bgd}}$) contribute nothing.

This definition for 3D objects has analogues in other dimensions. A 2D object exists only in one image slice, and the integral is over area or a number of pixels. For a 1D object (where the concept is most easily shown, as in Fig. 1) the integration is over one dimension.

In the simple case of a *uniform object* of intensity I^{obj} and volume V^{obj} then the Object Strength (Eq. (1)) is simply:

$$S^{\text{obj}} = (I^{\text{obj}} - I^{\text{bgd}}) V^{\text{obj}}. \quad (2)$$

Thus for a uniform object, the Object Strength is just the product of its excess intensity above the background and its size.

In a digital (discrete) image, values of intensity I_i are only available at specific locations. The Total EXcess Intensity (TEXI) of an object is defined as the sum of the excess intensity δ in each voxel:

$$\text{TEXI} = \sum_{i=1}^N (I_i - I^{\text{bgd}}) \quad (3)$$

N is the number of voxels over which the summation is carried out. Provided all the voxels with altered intensity are included, the exact region over which the summation takes place is unimportant. The partial volume effect is taken into account as follows. The intensity in voxel i is the sum of contributions from the object and the background:

$$I_i = I_i^{\text{obj}} v_i + I_{\text{bgd}} (1 - v_i), \quad (4)$$

where I_i^{obj} is the intrinsic intensity of the object (in the absence of partial volume effect) at voxel i , and v_i is the volume fraction of the object in that voxel ($0 < v_i < 1$). The absolute volume of object in the i th voxel is:

$$V_i = v_i V^{\text{voxel}}, \quad (5)$$

where V^{voxel} is the voxel size. Then from Eqs. (3–5), the total excess intensity is:

$$\text{TEXI} = \frac{1}{V^{\text{voxel}}} \sum_{i=1}^N (I_i^{\text{obj}} - I^{\text{bgd}}) V_i. \quad (6)$$

Comparing this with Eq. (1), it is seen that TEXI enables a discrete approximation to the Object Strength to be found:

$$S^{\text{obj}} \approx \text{TEXI} \delta \cdot \partial \lambda V^{\text{voxel}} \quad (7)$$

The approximation is valid even for the situation where the object has blurred edges that extend over several voxels (i.e. that the digital values fully sample the continuous function $I(\mathbf{r})$). Thus the edge of the object need not be defined, nor need it have sharp edges.

In the case of an object with sharp edges, that extend over less than 1 voxel, the nature of the MR imaging process is to represent correctly the zero spatial frequency

Fourier component (even though higher spatial frequencies will not be represented correctly). This component corresponds to the sum of intensities over (all relevant) space, and is the same as Eq. (3), therefore it is to be expected that object strength calculations from a discrete sample (i.e. a digital image) will always be correct (provided that all the Gibbs ringing has been included in the calculation).

In practical situations the background signal I^{bgd} will have to be determined as part of the measurement process; a convenient approach is as follows. A region of interest (ROI) is placed around the object (if it is two-dimensional, i.e. in a single slice), or a volume of interest (VOI) if three-dimensional, i.e. extending over several slices. The total signal intensity (TSI) is found by adding up the values of all the pixels or voxels within the ROI or VOI. TSI can usually be found simply, using existing image analysis software packages, by calculating the mean value I_m in the ROI or VOI, and multiplying by the number of samples (pixels or voxels) N

$$\text{TSI} = \sum_{i=1}^N I_i = N I_m = \text{TEXI} + N I^{\text{bgd}} \quad (8)$$

From Eq. (3) it is seen that TSI is simply related to TEXI. By measuring TSI at a range of sample sizes N (greater than the object size), it is expected to see a linear rise with N , of slope I_{bgd} , with vertical intercept equal to TEXI. Thus the background value need not be determined directly, but is determined automatically from a set of measurements of Total Signal Intensity vs ROI (or VOI) size.

The plot can be made more convenient to view by subtracting an estimated background value I^{ebgd} from each value of mean signal intensity. We define the term “estimated Total Excess Intensity” (eTEXI) by:

$$\begin{aligned} e\text{TEXI} &= \sum_{i=1}^N (I_i - I^{\text{ebgd}}) = N(I_m - I^{\text{ebgd}}) \\ &= \text{TEXI} + N(I^{\text{bgd}} - I^{\text{ebgd}}) \end{aligned} \quad (9)$$

(using Eq. (8)). TEXI is still given by the vertical intercept; however the plot is nearly horizontal (the slope is $I^{\text{bgd}} - I^{\text{ebgd}}$) and it is easier to see whether the data follow the expected behaviour. Thus data for eTEXI measured at various ROI or VOI sizes N , with an estimated background value I^{ebgd} , give TEXI, and I^{bgd} is also provided. Although the computation required for the eTEXI plot (Eq. (9)) is a little more than for the basic TSI plot (Eq. (8)), (since the estimated background I^{ebgd} is subtracted in Eq. (9) but not in Eq. (8)), the graphical presentation that is possible (see Fig. 3 below) does add insight into the process.

In practical situations, the (implicit) estimation of the background intensity might be limited by the presence of noise (although the larger ROI's would probably overcome this, leaving noise within the object as dominating

the uncertainty in the OS estimate). The presence of other nearby objects, or other heterogeneities, could also limit how large the ROI's could be made, and thus how well the background could be characterised.

Methods

Reproducibility of measurements of MR lesion object strength and lesion size

Thirty discrete white-matter MR lesions were identified in patients with multiple sclerosis [5]. Each lesion was reported in a single slice only. These were imaged using a spin echo sequence with TR=2000 ms, TE=34 ms, pixel size 0.96 mm, slice thickness 5 mm. Each lesion was reported by three observers twice, in two separate sessions separated by about a week. Two of these (observers 1 and 2) were neuroimaging research fellows, accustomed to the computerised delineation of MS lesions on MR images; the third was a relatively inexperienced observer. A set of 7 ROI's was drawn around each lesion (as seen in a single slice – see Fig. 2), and for each ROI, its area and mean signal value were recorded. The smallest ROI was within the visible lesion; subsequent ROI's were of increasing size, and restricted to the uniform-appearing tissue around the lesion. The second ROI (#2) was placed on the lesion boundary, as far as possible, and used to estimate the lesion area. The generation of ROI #2 was carried using a semi-automatic contouring program Dispimage [7] (<http://www.medphys.ucl.ac.uk/~dlp/dispim.htm>). In this method, a seed pixel is identified on the lesion edge, and then a contour is generated automatically. The other ROI's (#1 and #3–7) were drawn manually. The largest ROI (#7) was typically 5–7 times larger than the nominal lesion area (ROI #2 - see Figs. 2, 3 & 8). The two-dimensional lesion object strength was estimated from the eTEXI plot. The linear regression gave the standard error (SE) in the estimate of TEXI, and a RMS residual error, both of which were used to monitor the quality of the data. The eTEXI plot was inspected to determine the linear portion for regression; usually ROI numbers 4–7 were used. Intra-observer variability in estimates of lesion area and lesion object strength were calculated. The fractional (%) difference between the two measurements by the same observer was used as a simple measure of reproducibility.

Accuracy of MR object strength measurements on OCCA artificial lesions

The Oblique Cylinder Contrast Adjusted (OCCA) phantom [3] provides uniform artificial lesions of known volume and realistic appearance. The lesions consist of plastic cylinders of known diameter and length in a water bath. These are mounted obliquely to the imaging plane (so that partial volume effects are realistic). For MR images, the contrast is inverted (to make the lesions bright against a dark background), and noise is added

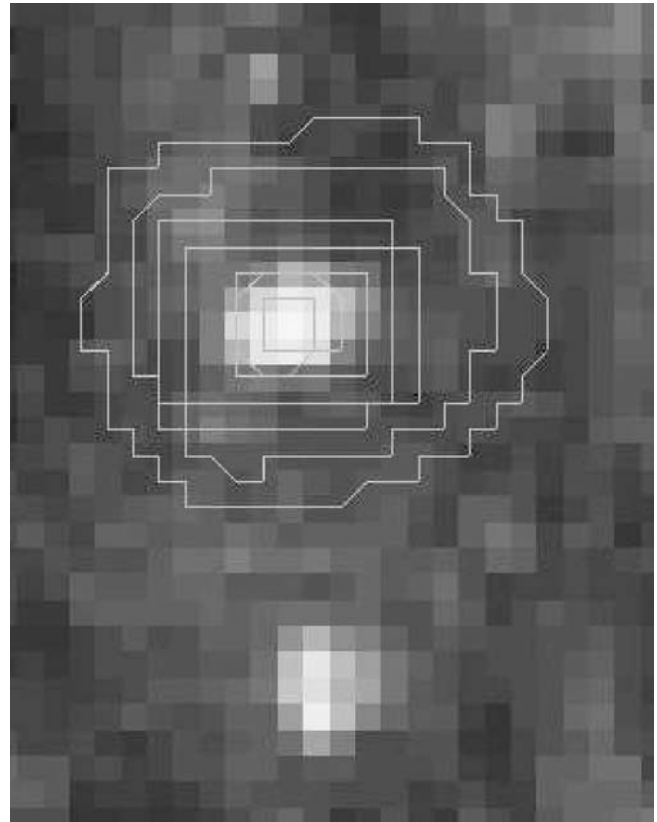


Fig. 2 Example of the set of 7 ROI's drawn round a small MS lesion. Region#2 (the second smallest) is the contour that was generated semi-automatically; this estimates the boundary of the lesion

(so that contrast-to-noise ratios are realistic). Nine lesions, with volume 0.3–6.1 ml, (total volume 19.9 ml), were imaged using 5 mm thick slices. The contrast was adjusted to give 30% lesion to background signal ratio and 20:1 contrast to noise ratio.

Lesion volume was estimated [6] from values of three-dimensional object strength as follows. The 3D strength was measured by one observer for each lesion by summing the contributions from each slice in which the lesion was visible. The 2D strength was measured in units of Signal Intensity \times mm²; the 3D strength was obtained by adding the 2D values and multiplying by the slice thickness, giving units of Signal Intensity \times ml. The mean signal in the background and in a large lesion were also measured, to give estimates of I^{bgd} and I^{obj} . From these, lesion volume was estimated, using Eq. (2) and knowing that the lesions were intrinsically uniform.

Results

An example of TEXI measurements is shown in Table 1 and plotted in Fig. 3. For each of the 7 ROI's, eTEXI is calculated and plotted. The mean value is also shown, decreasing with ROI size.

Table 1 Example of generation of data for 2D eTEXI (estimated Total EXcess Intensity) plot shown in Fig. 3, using estimated background intensity $I^{\text{bgd}} = 195$

ROI#	Measured ROI area (N) (pixels)	Measured mean signal in ROI (I_m)	Total signal intensity TSI= $N\delta \cdot I_m(a)$	eTEXI= $N(I_m - I^{\text{bgd}})$ (a)
1	16.7	237.2	3961	705
2	34.3	231.1	7927	1238
3	47.5	224.9	10683	1420
4	63.3	218.8	13850	1506
5	91.4	212.9	19459	1636
6	127.4	209.2	26652	1809
7	174.0	206.8	35983	2053

(a) Regression of TSI versus N, or of eTEXI vs N, both give vertical intercept $\text{TEXI} = 1186$ (see Fig. 3 and Eqs. (8) and (9)). However the eTEXI plot is more convenient, since the slope is near zero

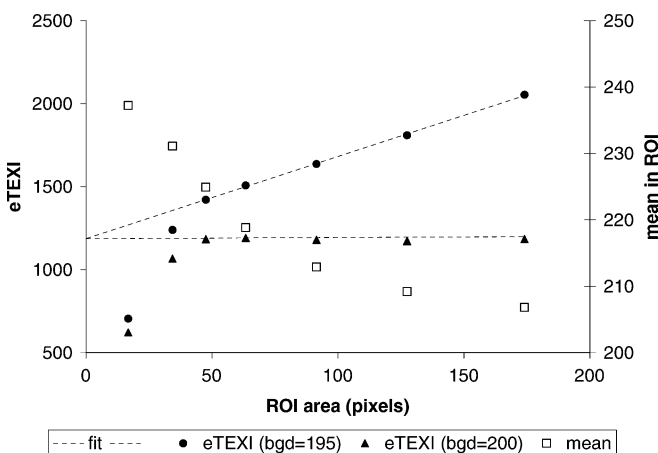


Fig. 3 Example of an eTEXI (estimated TEXI) plot, for a set of 7 ROI's of increasing size drawn around an isolated lesion (see Table 1). The second ROI (area 34 pixels in this example) was intended to represent the border of the lesion. The mean value (*right hand axis*) is larger for ROI #1 (area 17 pixels), showing that the lesion is nonuniform and has no well-defined mean value. The eTEXI plots show that there is significant lesion intensity outside the apparent border (ROI #2), since the data only rise to meet the fitted straight line at ROI #3 (48 pixels). Regression of the eTEXI plots, using the linear portions (ROI's #4–7), with two different background estimates ($I^{\text{bgd}} = 195$ and 200) both gave the same vertical intercept $\text{TEXI}^0 = 1186$. (For comparison, the TSI regression (Eq. (8)) gives compatible results: estimated background = 200.0, $\text{TEXI}^0 = 1186$)

Reproducibility of measurements of lesion object strength and lesion size

In the reproducibility study, lesion areas ranged from 11 pixels to 119 pixels (median 24, mean 33). An analysis of the intra-observer differences is shown in Table 2. The standard error of the TEXI estimates was generally acceptable (median value 4.0%); however a few were poor (maximum value 260%). Therefore the analysis was re-

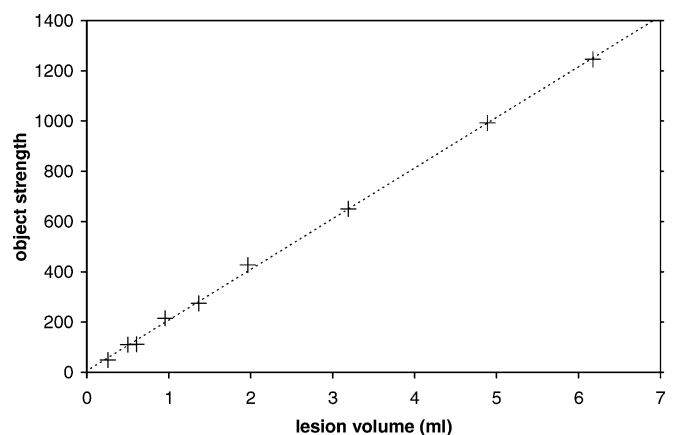


Fig. 4 In artificial OCCA lesions, correlation between known lesion volume and measured object strength

peated with the 10/90 datasets having a SE of $\geq 10\%$ being excluded (also shown in Table 2). The maximum difference in repeated OS measurements was then 30%, and in 30/80 lesion reports the OS measurement was more reproducible than the area measurement.

Accuracy of object strength measurements on OCCA artificial lesions

Object strength correlated extremely closely with known lesion volume (Fig. 4), for the nine lesions. Linear regression of lesion object strength vs. lesion volume gave a correlation coefficient of 0.999, a slope of 202 ± 2 (\pm denotes standard error), and a vertical intercept of 7 ± 14 .

Measured background and lesion signal intensities were $I^{\text{bgd}} = 635 \pm 5$ (estimated 95% confidence limits) and $I^{\text{obj}} = 840 \pm 2$. Thus within the confidence limits of the regression, the slope of the regression was as predicted by Eq. (2) (i.e. $I^{\text{obj}} - I^{\text{bgd}}$) and the vertical intercept was zero.

Table 2 Intra-observer reproducibility of lesion Object Strength (OS) and lesion area measurements in 30 MR lesion images [5]. Three observers each reported 30 lesions, using both the OS and area methods. All measurements were repeated. The differences between repeated measurements (for a given observer) were analysed

	Observer #1 (experienced)		Observer #2 (experienced)		Observer #3 (inexperienced)		All 3 observers ^{a1}		Observers#1 ^{a2} (experienced)	
	OS	Area	OS	Area	OS	Area	OS	Area	OS	Area
Absolute fractional differences (%) ^b										
Median	6	0	6	0	11 [9] ^c	13	9 [7] ^c	5	6 [6] ^c	0
Mean	9	5	8	8	18 [10] ^c	16	11 [9] ^c	10	8 [8] ^c	7
Maximum	30	22	21	35	123 [24] ^c	61	123 [30] ^c	61	30 [30] ^c	35
Number of lesions										
Δ area=0 ^d	20/30 [20/29] ^c		15/30 [15/30] ^c		5/30 [5/21] ^c		40/90 [40/80] ^c		35/60 [35/59] ^c	
Δ OS> Δ area ^e	24/30 [24/29] ^c		18/30 [18/30] ^c		14/30 [7/21] ^c		56/90 [49/80] ^c		42/60 [42/59] ^c	
Δ OS< Δ area ^f	5/30 [4/29] ^c		12/30 [12/30] ^c		16/30 [14/21] ^c		33/90 [30/80] ^c		17/60 [16/59] ^c	

^{a1} Pooled from 90 observations (3 observers each measuring 30 lesions)

^{a2} Pooled from 60 observations (2 experienced observers each measuring 30 lesions)

^b Percentage difference between the two measurements by the same observer, measured for each of 30 lesions

^c Values calculated excluding all fits with $TE\% \geq 10\%$ are shown in [square brackets]

^d Number of lesions where *same area* was reported in both sessions

^e Number of lesions where % difference in object strength was *greater than* % difference in area

^f Number of lesions where % difference in object strength was *less than* % difference in area

Lesion volume estimates were very accurate (median absolute error 0.05 ml; median fractional error 6%). Total lesion volume error was 0.03 ml (0.16%). Regression of measured volume vs known volume gave a correlation coefficient of 0.999, slope=0.983 (se=0.011), intercept 0.032 (se=0.034). Using a background value of $I^{bgd} = 640$ (instead of 635) increased the estimated total volume by only 0.5 ml (2.5%).

Discussion

In validating the new quantity of object strength, two important considerations are accuracy and precision. Accuracy (closeness to the true value) is clearly acceptable for Object Strength (see Fig. 4, and bearing in mind the results of the artificial lesion measurements), whilst for conventional area measurements it is clearly weak in the presence of partial volume (see Fig. 2, and as shown by the OCCA lesion study [3]). Precision for Object Strength is reasonable (Table 2, and see below), particularly as it has been compared with a semi-automatic method, and no rescanning was carried out.

The strong dependence, in small objects, of mean value on ROI size (Fig. 3) suggest that conventional estimates of mean lesion intensity are probably flawed, since there is no well-defined value, just a steady change towards the background value as the ROI size is increased. Similarly, conventional estimates of volume are unreliable.

The OCCA validation (Fig. 4) shows that the concept behind object strength has been verified. This concept is that a small isolated object, in a homogeneous background, subject to large partial volume effects, can be accurately characterised using a set of ROI's larger than the object. The object need not be uniform (although in this example it was uniform, and in any case it must be either all brighter or all darker than the surrounding background). Under some conditions, the estimates of lesion volume can be far more accurate than those obtained by drawing single ROI's around the object, as measured in a previous study [3]. In that study, a large between-observer variation was seen, and reported volumes also depended on the object contrast.

In estimating precision (i.e. how repeatable the measurements were), many of the area estimates (40/90) were identical in the repeat (second) session, probably because two of the observers were very experienced at making these measurements. This reproducibility estimate for the ROI area is probably unfairly optimistic, as happens with any method that is largely automated, since it includes only variation from analysis, but not that from scanning. If the image data had been collected again, and reproducibility measured from the repeated dataset, reproducibility performance would probably have been worse than measured in this study (because of the effects of repositioning and because image noise realisations are not identical with repeated scanning). Indeed the semi-automatic contouring method is such that if the

same pixel is picked as the seed, an identical ROI will be produced.

The three observers differ widely from each other in how well they could estimate both lesion size and object strength (Table 2). In discussion it became clear that they had developed different strategies for drawing the ROI's. In particular, their strategies differed in two important respects: (1) how to treat cases where there was adjacent grey matter which could give a non-uniform background, and (2) what range of ROI sizes to create for the object strength estimates. Observer 3 (the least experienced) had consistently worse fits, indicating a more naïve approach to ROI creation, and his performance was generally worse than the other two, for both OS and area (see Table 2). Removing the poor TEXI plots ($SE \geq 10\%$), where the model clearly was not valid, improved the performance and shows that the Object Strength concept must be used with an awareness of its limitations. With increased familiarity and training the reproducibility of the object strength estimates would probably improve. Looking at the two experienced observers alone (Table 2, right hand column), OS and area had similar values of mean and maximum difference.

In spite of these initial difficulties, in more than one-third of the lesion reports (33/90; or 30/80 of the reports where a good TEXI fit was obtained) object strength was more reproducible than conventional lesion area, and indicates its potential value.

Although we have not explicitly measured random errors by analysis of repeated scanning, the nine objects (shown in Fig. 4) are subjected to independent samples of noise, and thus the scatter from the line is indicative of the small random error associated with the Object Strength measurements.

The concept of brightness area product (BAP) is related to that of Object Strength. It has been recognised in cardiac imaging for many years [8], and is incorporated into the Analyze image analysis package [9], where it is defined as the sum of the pixel values above a threshold in a region. However its formal relation to object size and amplitude, in the presence of partial volume effects, has not been evaluated, and it does not take account of the background in the way that the Object Strength formalism does.

The time to generate the eTEXI plots is currently about 5 min per lesion, including drawing ROI's and setting up the regression. This is feasible for a single object extending over a few slices; for multiple lesions this may be too large to make the procedure available for routine use. An automated procedure for generating the ROI's could be based on identifying a seed point in the lesion. The linear portion in the regression could be identified, a test made for goodness of fit, and lesion portions seen in adjacent slices connected. This would speed up the process, and also enable some of the issues around selection of

ROI's in the presence of background heterogeneity to be explored. Reproducibility would probably also improve (just as automation of contour generation has improved the reproducibility of lesion volume measurements).

The object strength measurement technique is vulnerable in the situation of a non-uniform background, or of a background consisting of more than one distinct tissue (for example a white matter lesion close to grey matter or CSF). Such a heterogeneous background would cause problems with any technique designed to characterise a small abnormality, since there must be a notion of what is normal before this can be done. Nonetheless, the characterisation of small lesions on uniform backgrounds is probably the first area to exploit in further exploration of the Object Strength technique. Nonuniform and heterogeneous backgrounds may be able to be dealt with in the future by more sophisticated approaches (for example segmentation of a background containing two tissues).

Potential applications of the Object Strength concept in MR include small isolated lesions of multiple sclerosis, tumours, subcortical vascular lesions (e.g. from transient ischemic attack), and lesions in specific fibre tracts (e.g. pyramidal tracts, for the delineation of Wallerian degeneration). Small objects such as the optic nerve and spinal cord may also be amenable to this approach, although the lack of an obvious uniform background presents difficulties, particularly in the optic nerve. In some cases lesion Object Strength may be biologically more appropriate than conventional measures such as intensity or apparent size, since it combines measures of lesion hyper-intensity (or hypo-intensity) with lesion size. It may be possible to alter MR data collection procedures to use larger voxels (since partial volume effects are much less important), giving improvements in signal-to-noise ratio or data collection time.

In single-voxel MR spectroscopy it is often hard to place the relatively large spectroscopic voxel entirely within a lesion; if it is possible, then some lesion is excluded, and also the resulting small voxel size may compromise signal-to-noise ratio; for both reasons the resulting sensitivity is reduced. An alternative approach may be to collect spectra from a set of voxels that are *larger* than the lesion (one that just includes the lesion, and several larger ones that include varying amounts of background, similar to the ROI scheme in Fig. 2). A plot of total amount of metabolite vs voxel volume would give an estimate of the total metabolite excess or deficiency in the lesion, which is one of the biologically relevant parameters. The total examination time need not be excessive, since larger volumes need far fewer signal averages (for a given amount of noise, the number of averages required is inversely proportional to the square of the voxel volume).

The principle measure considered here has been object strength, which has units of signal intensity multi-

plied by volume. It would be desirable to have measures which are independent of the scanner settings (such as gain or sequence contrast). If the object is known to be uniform and of known intensity, its size can be found (as we did for the OCCA phantom), giving the desired independence of the scanner gain. Alternatively the signal intensities could all be scaled such that the background intensity becomes unity (i.e. the object strength is measured relative to the background), and object strength would then be an effective volume. The third possible measure is one of object intensity, if an independent high-resolution estimate of size can be obtained. For example the MR spectroscopic strength of a lesion could be measured; division by its volume would give a measure corresponding to the mean alteration in metabolite concentration.

In conclusion, the object strength approach circumvents the problems of partial volume and fuzzy borders in characterising small objects of arbitrary heterogeneity. This pilot study (proof of concept) has verified the theory and suggests it is reliable enough to warrant further investigation and refinement, in imaging and possibly in spectroscopy.

Acknowledgements The Multiple Sclerosis Society of Great Britain and Northern Ireland generously supported NS, GJB and the MRI scanner. The European Union supported the MAGNIMS Magnetic Resonance and Multiple Sclerosis network through contract ERB-CHRXCT940684. Dr Dan Tozer critically read the manuscript, and assisted in generating Fig. 2.

References

1. Filippi M, Dousset V, McFarland HF, Miller DH, Grossman RI (2002) Role of magnetic resonance imaging in the diagnosis and monitoring of multiple sclerosis: consensus report of the White Matter Study Group. *J Magn Reson Imaging* 15(5):499–504
2. Barker GJ, Schreiber W, Gass A, Ranjeva JP, Campi A, van Waesberghe JH, Franconi JM, Watt HC, Tofts PS (2005) A standardised method for measuring magnetisation transfer ratio on MR imagers from different manufacturers - the EuroMT sequence. *MAGMA* 2005 18(2):76–80
3. Tofts PS, Barker GJ, Filippi M, Gawne-Cain M, Lai M (1997) An oblique cylinder contrast-adjusted (OCCA) phantom to measure the accuracy of MRI brain lesion volume estimation schemes in multiple sclerosis. *Magn Reson Imaging* 15(2):183–192
4. Lucchinetti C, Bruck W, Parisi J, Scheithauer B, Rodriguez M, Lassmann H (2000) Heterogeneity of multiple sclerosis lesions: implication for the pathogenesis of demyelination. *Ann Neurol* 47:707–717
5. Tofts PS, Silver NC, Barker GJ, Lai M, Gass A (1997) Object strength – a reproducible lesion measure that is insensitive to partial volume errors. In: *Proc Intl Soc Mag Reson Med*, 5th annual meeting, Vancouver, 49
6. Tofts PS (1998) Object strength correlates closely with OCCA MS brain phantom lesion volume, and can accurately predict lesion volume. In: *Proc Intl Soc Mag Reson Med*, 6th annual meeting, Sydney, 2074
7. Plummer DL (1992) DispImage a display and analysis tool for medical images. *Rivista Di Neuroradiologica* 5:489–495
8. Scanlan JG, Gustafson DE, Chevalier PA, Robb RA, Ritman EL (1980) Evaluation of ischaemic heart disease with a prototype volume imaging computed tomography (CT) scanner: preliminary experiments. *Am J Cardiol* 46:1263
9. Robb RA (2000) *Biomedical Imaging, Visualization and Analysis*. Wiley-Liss, New York